E3S Web of Conferences **664**, 01005 (2025) https://doi.org/10.1051/e3sconf/202566401005
ISSAT 2025

Thermal diagnostics of high-current EV components with an artificial neural network model

Safarudin Gazali Herawan[1*], *Sharon* Yemima[1], *Azqy Nur Farenzy* Saputra[1], *Bangkit Pramesta* Yulianto[1], *Henry Ananda* Chang[1], *Heri* Ngarianto[1], *Rida* Zuraida[1], and *Mohd Zaid Bin* Akop[2]

[1] Industrial Engineering Department, Faculty of Engineering Bina Nusantara University, Jakarta, Indonesia 11480
[2] Faculty of Mechanical Technology and Engineering, Universiti Teknikal Malaysia Melaka, Melaka, 76100, Malaysia

Abstract. The increasing complexity of thermal management in Electric Vehicle (EV) powertrains necessitates accurate and scalable predictive models for monitoring cable and connector temperatures. This study investigates the performance of a lightweight Artificial Neural Network (ANN) for predicting main switch, connector, and motor cable temperatures using nine input features encompassing electrical and thermal parameters. Model evaluation was conducted against Support Vector Machine (SVM) and linear regression baselines using R^2, MAE, and RMSE metrics. Results show that the ANN consistently outperformed benchmark models, achieving R^2 values above 0.96 and maintaining temperature deviations within ±2.5 °C across all test scenarios. Unlike SVM and linear regression, which required separate models for each output, the ANN successfully predicted multiple outputs within a single framework, demonstrating greater scalability. Feature importance analysis identified battery temperature and post-switch cable temperature as dominant predictors, findings corroborated by high-resolution thermal imaging that confirmed localized heating in these regions. Despite the strong performance, limitations include a relatively small dataset and laboratory-based validation, which may restrict generalizability. The outcomes highlight the ANN's potential for embedded real-time monitoring and predictive maintenance in EV thermal management, while underscoring the need for future research using larger, more diverse, and field-derived datasets.

1 Introduction

Maintaining the thermal stability of electrical systems is critical to ensuring operational safety and performance. Components such as main switchboards, connectors, and motor cables are especially prone to failure when exposed to excessive heat. These failures can result in system malfunctions, reduced efficiency, and in extreme cases, safety hazards. This is particularly

* Corresponding author: safarudin.gazali@binus.edu

true in environments where systems are subjected to high loads or extended operation. As numerous studies indicate, thermal failures often stem from prolonged overloading or insufficient dissipation mechanisms [1,2].

Thermal failure mechanisms are diverse. Overloading remains a key contributor, as electrical components operated beyond their design limits generate excessive heat, accelerating material fatigue and failure [1,2]. Thermal aging also degrades insulation materials like crosslinked polyethylene (XLPE), which under continuous high-temperature exposure suffer mechanical deterioration and heightened failure risk [3-5]. Environmental conditions—such as elevated ambient temperature, moisture, and chemical exposure—further exacerbate these effects [2,6].

Traditionally, thermal monitoring relies on reactive methods. Infrared thermography and thermal imaging are widely used to identify surface temperature anomalies [1,7,8]. While effective for detecting existing faults, these tools are not designed to predict failures before they occur. Capacitance testing and dielectric loss assessments provide deeper insight into insulation health but are less practical for real-time monitoring and may lack temporal resolution [9].

The emergence of predictive maintenance, especially through data-driven techniques, has created new possibilities for thermal monitoring. Machine learning models—particularly Artificial Neural Networks (ANNs)—can capture complex, nonlinear relationships within electrical and thermal data, allowing prediction of fault-prone conditions before they escalate [8, 10]. In smart grids, ANNs enhance system reliability by forecasting thermal anomalies, reducing maintenance costs and downtime [11,12].

Research has demonstrated the effectiveness of ANNs in identifying faults across electrical networks, including those in renewable energy and hybrid systems [13-15]. Their adaptive capabilities are advantageous in dynamic operating conditions where conventional rule-based models may struggle. This shift from reactive to predictive maintenance highlights the value of flexible, learning-based models for monitoring critical components.

Despite their potential, implementing machine learning in real-time embedded systems remains challenging. Deep ANN architectures often demand significant computational power and memory, which are not always available in embedded environments [16,17]. Moreover, model performance depends heavily on the quality and relevance of training datasets. Insufficient or biased data can cause models to overfit or generalize poorly [15,17]. Integrating these models into existing infrastructure is also complex due to compatibility issues with legacy systems.

To address these constraints, researchers are exploring shallow feedforward neural networks using logistic sigmoid activation functions. These models offer several advantages, including interpretable outputs, smooth convergence through gradient descent, and efficient operation on constrained hardware [18,19]. Their structure is conceptually grounded in biological neural mechanisms, which contributes to their appeal in interpretable modeling.

However, shallow networks are not without limitations. Although they perform well in simple predictive tasks like temperature forecasting, they lack the depth to capture complex patterns that deeper models can handle. Deep networks benefit from hierarchical feature learning, enabling them to model high-dimensional relationships more effectively [20-22]. Nevertheless, in applications where computational simplicity and real-time operation are priorities, shallow ANNs remain a viable alternative.

This study introduces a compact feedforward ANN that leverages logistic sigmoid activation to predict the temperatures of key components—main switch, connector, and motor cable—in an EV electrical system. The network uses nine inputs, comprising voltage ratio, current, battery capacity ratio, and temperatures from various subsystems. Its architecture is deliberately minimal, allowing fast, efficient computation suitable for embedded systems.

2 Methodology

This research adopts an empirical strategy aimed at analysing thermal behavior in high-current Electric Vehicle (EV) power cable systems under operational simulations. The approach encompasses the design of a laboratory-scale experimental model, a rigorous protocol for data acquisition, and systematic thermal profiling of multiple cable components. The methodology is motivated by prior research that stresses the necessity of identifying localized thermal hotspots in EV power distribution systems, especially under conditions involving high-speed charging and large-scale energy transfer [2, 3, 6].

2.1 Experimental arrangement

The experimental framework replicates a high-power EV drivetrain environment within a controlled laboratory setup. As outlined in Fig. 1, a brushless DC (BLDC) motor is mechanically linked to a braking system driven by an electric actuator, with operational input managed via a throttle mechanism simulating real-life acceleration conditions. The motor is governed by a VOTOL controller, interfaced with a custom-built battery assembly comprising thirteen serially connected battery cells. This battery system integrates a smart Battery Management System (BMS), which communicates through Bluetooth with the Jikong smartphone application, enabling real-time tracking of both individual cell voltages and aggregate battery temperatures.

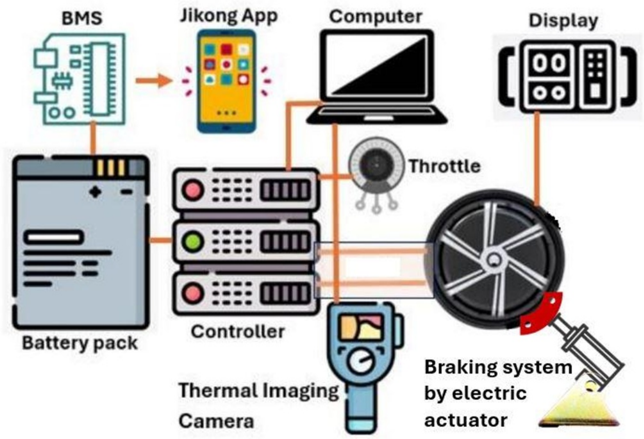

Fig. 1. A schematic overview of the test configuration.

The setup includes a multifunction display module that presents operational parameters such as vehicle speed (km/h), total distance covered (km), state of battery charge, and the motor's current thermal state. Simultaneously, voltage, current, and power data—along with temperature measurements—are transmitted from the motor controller to a connected PC, enabling dynamic logging and visualization. Comprehensive hardware specifications are documented in Table 1, and Fig. 2 depicts the physical test bench layout, illustrating the integration and spatial configuration of key electrical subsystems under simulated driving conditions. Additionally, Fig. 3 showcases the electric-actuated braking assembly employed to introduce variable loads.

Table 1. Specifications of Experimental Components

No.	Component	Specification
1	BLDC Motor	1500 W
2	SiAECOSYS VOTOL Controller	50 A
3	Battery Pack (13s6p, 78 cells total)	48 V, 15 A
4	Throttle	Potentiometer with spring return
5	Display	RPM, speed, and battery capacity indicators
6	Jikong BMS	Voltage and temperature sensing for 13 cells
7	InfiRay P2 Pro Thermal Camera	Range: -20°C to 550°C; Accuracy: ±2°C

Figure 2 depicts the assembled rig used for thermal experimentation, while Fig. 3 details the electric actuator-based braking unit.

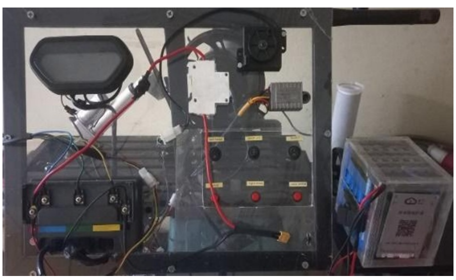

Fig. 2. The experimental rig for conducting test.

Fig. 3. The braking mechanism.

The design of this experimental platform draws from recent advancements in thermal diagnostic methodologies, which emphasize the critical importance of integrating spatially-resolved sensor data [9, 11]. Accordingly, the system is equipped with a high-resolution infrared thermal camera that enables non-contact temperature measurements across multiple cable points and critical components with fine granularity.

2.2 Experimental protocol

Experiments were executed at the Manufacturing Process Laboratory, Binus University Syahdan campus, with the aim of simulating the thermal stresses typical of real-world EV operation. The testing procedure involved applying maximum throttle input and incrementally increasing braking force using the electric actuator to mimic variable operational loads. Load conditions were adjusted in predefined steps—0%, 20%, 40%, 60%, 80%, and above 80%—to simulate a range of current draw scenarios and induce corresponding thermal effects across the system.

During each test iteration, temperature readings were captured from strategically selected locations using the thermal imaging device. These key points included the motor controller, battery pack, DC-DC voltage regulator, main power switch, and the connector terminals. Additional thermal data were acquired from the negative terminal (ground cable), both upstream and downstream segments of the main power cable, and the motor cable itself.

Thermal images generated throughout testing yielded detailed heat maps, enabling spatial analysis of heat concentration zones and thermal gradients. These were supplemented with real-time electrical measurements—such as current, voltage, and power draw—which contextualized the thermal responses under varying operational intensities. This method aligns with findings reported in prior literature that emphasize the dynamic interaction between electrical loading and temperature rise as critical to component degradation and system reliability [1, 2].

By progressively escalating load conditions and collecting corresponding thermal and electrical data, the methodology enabled precise identification of abnormal heating patterns and critical temperature peaks. In particular, comparative assessments were made between input and output temperatures across the main switch and cable connections—areas repeatedly highlighted in prior research as thermal risk zones [4, 5].

This structured approach facilitated the diagnosis of specific cable sections and subsystems that exhibit significant thermal stress. Such focused diagnostics form the basis for future design enhancements. Echoing the simulation-driven models discussed in recent work, the dataset acquired from this study is intended for use in the calibration and validation of predictive thermal models tailored to EV power distribution [11]. Although active cooling technologies were not introduced in this investigation, the baseline thermal data obtained serve as a crucial reference for optimizing future thermal management solutions.

The empirical approach simulates thermal behavior in high-current EV cable systems using a laboratory-scale test rig. Data were collected at over multiple runs, each 5 minutes, under varying load conditions (0% to >80%). The resulting dataset comprises 14 samples, partitioned into training (70%), validation (15%), and testing (15%) sets. Preprocessing involved normalization and outlier removal. In addition to the proposed ANN, benchmark models—SVM and linear regression—were trained using identical input features to contextualize performance. Model evaluation included R^2, MAE, and RMSE metrics.

3 Results and discussion

The experimental investigation and model evaluation were conducted to examine the predictive capability of a lightweight artificial neural network (ANN) in estimating temperature dynamics across high-current Electric Vehicle (EV) power cable systems. The analysis focused on three primary thermal outputs—main switch temperature, connector temperature, and motor cable temperature—derived from nine carefully selected input features. These included electrical parameters such as voltage ratio, current, and battery capacity ratio, as well as six thermal variables representing component-level conditions across the powertrain. The input selection strategy is consistent with established thermal analysis practices in EV systems, where multi-source signals are recognized as essential for robust predictive modeling [1,2].

Visualization of the model outputs reveals a strong correspondence between predicted and observed temperatures across all datasets. As shown in Fig. 4, ANN-based predictions for the main switch demonstrate exceptional fidelity, remaining within ±2 °C of actual values over the full throttle spectrum. Achieving this narrow margin of error is non-trivial, given the known challenges in maintaining real-time prediction accuracy under rapidly changing load conditions [3,4]. The coefficient of determination (R^2) of 0.978 further underscores the ANN's reliability under baseline operating conditions. Such performance highlights the ANN's capacity not only for interpolation within the training domain but also for generalization across unseen operating states, a critical requirement for embedded diagnostic applications.

Model comparisons provide additional insight. Table 2 summarizes the performance metrics for ANN, support vector machine (SVM), and linear regression models. While SVM models were tuned with kernel variations—RBF for the main switch and motor cable, polynomial for the connector—the ANN consistently outperformed them on all metrics. The ANN achieved higher R^2 values and lower MAE scores, reinforcing its superior accuracy and reduced error propagation. Beyond accuracy, a key advantage of the ANN lies in its multi-output capability: it is able to predict all three thermal outputs simultaneously using a single network. By contrast, SVM and linear regression approaches required three separate models, limiting efficiency and scalability. This result emphasizes the suitability of ANN frameworks for complex, multi-dimensional tasks in EV thermal management.

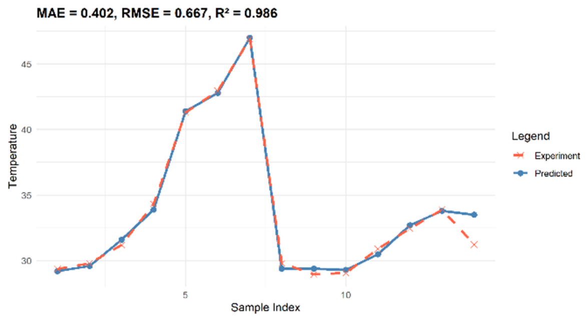

Fig. 4. ANN temperature prediction vs main switch.

Table 2. Model evaluation included R^2, MAE, and RMSE metrics for ANN, SVM, and Linear regression.

Model	**Component**	**R^2**	**MSE**	**RMSE**
ANN	Main switch	0,986	0,402	0,667
	Connector	0,995	0,138	0,204
	Motor cable	0,919	0,4	0,812
SVM	Main switch	0,24	0,91	0,73
	Connector	2,04	0,46	1,09
	Motor cable	1,47	2,14	5,42
Linear regression	Main switch	0,19	0,07	-6,29
	Connector	2,17	4,6	29,39
	Motor cable	1,47	2,14	5,42

Feature importance analysis further illustrates the interpretability of the model. Among the nine input variables, battery temperature and main switch cable temperature emerged as dominant predictors, with high weight magnitudes across multiple hidden neurons. For instance, in neuron h_5, the coefficient for post-switch cable temperature reached 1.036, while coefficients for battery temperature exceeded 1.0 in other neurons. These results converge with prior studies that identify battery heating and switch-induced conduction losses as key drivers of localized thermal stress in EV powertrains [4,5]. The significance of these features was validated through high-resolution thermal imaging, which revealed concentrated hot spots around the main switch and connector terminals. Such agreement between statistical modeling and empirical imaging enhances confidence in the model's predictive validity, while also underscoring the central role of thermal coupling in EV reliability.

The robustness of the ANN is further evidenced in the connector dataset, particularly under variable braking loads. Figure 5 demonstrates that predicted connector temperatures closely follow measured trends, with deviations constrained within ±2.5 °C. The R^2 value of 0.969 affirms that the ANN can capture nonlinearities associated with transient thermal spikes—a feature often elusive in traditional regression-based models. Similar trends were observed in the motor cable dataset (Fig. 6), where the ANN achieved an R^2 of 0.962. Although slightly lower than for the main switch and connector, this still represents an excellent fit given the complexity of rapid cable heating during high-load conditions. Such results are consistent with literature that highlights the challenges of modeling cable insulation degradation and localized thermal fluctuations under electrical overstress [2,10].

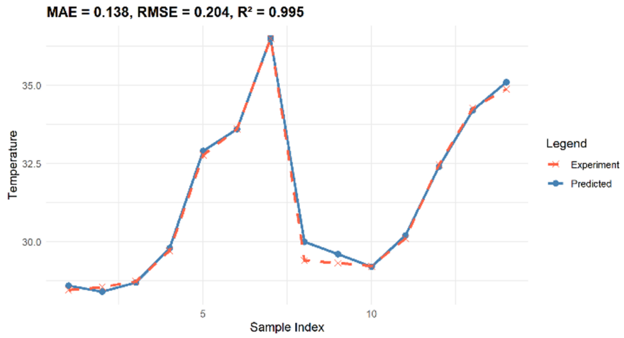

Fig. 5. ANN temperature prediction vs connector.

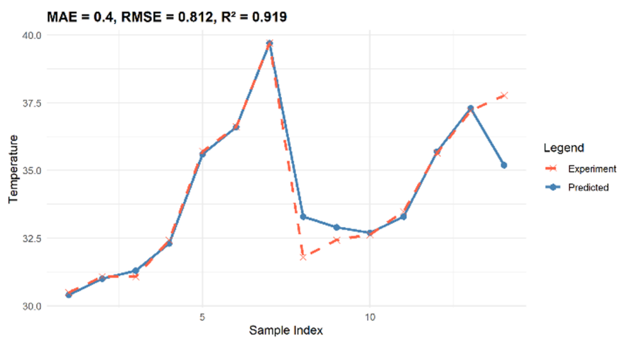

Fig. 6. ANN temperature prediction vs motor cables.

Overall, the ANN consistently delivered R^2 values above 0.96 across all outputs, exceeding benchmarks reported for shallow architectures in comparable applications. For example, Hamdan and Roach [18] describes neural network implementations with logistic sigmoid activation achieving R^2 values of 0.85–0.94 in dynamic environments. The higher predictive fidelity in this study may be attributed to both the curated feature set—balancing electrical and thermal signals—and the compact hidden-layer configuration, which minimized overfitting while preserving model generalization.

At the algorithmic level, the model's design can be traced through its logistic sigmoid hidden layer and identity-activated output neurons. The hidden layer, comprising five neurons, assigned particularly high positive weights to battery and post-switch cable temperatures, confirming their influence. Conversely, inputs such as voltage ratio and current displayed mixed contributions, reflecting their more complex interactions with dynamic load cycles. This transparency into weight distributions provides an interpretative lens often absent in black-box ANN discussions, aligning with recent calls for interpretable machine learning in safety-critical applications [7,9]. The detail of the algorithm can be shown as follows:

1. Activation Function
The logistic sigmoid activation function is defined as:
$f(z) = 1 / (1 + e^{-z})$

2. Hidden Layer – 5 Neurons (Activation: Logistic Sigmoid)
Hidden Neuron h_1
$z = -0.578 \cdot V\_ratio - 0.389 \cdot I - 1.031 \cdot Battery\_capacity\_ratio + 0.036 \cdot Controller\_Temp + 1.056 \cdot Battery\_Temp + 0.791 \cdot Regulator\_Temp + 0.489 \cdot Ground\_Cable\_Temp + 0.392 \cdot PowerCable\_Before\_Temp + 0.286 \cdot PowerCable\_After\_Temp - 1.031$
$h_1 = f(z)$
Hidden Neuron h_2
$z = -0.326 \cdot V\_ratio - 0.166 \cdot I + 0.089 \cdot Battery\_capacity\_ratio + 0.062 \cdot Controller\_Temp + 0.396 \cdot Battery\_Temp + 0.099 \cdot Regulator\_Temp + 0.186 \cdot Ground\_Cable\_Temp + 0.325 \cdot PowerCable\_Before\_Temp + 0.572 \cdot PowerCable\_After\_Temp - 0.194$
$h_2 = f(z)$
Hidden Neuron h_3
$z = -0.041 \cdot V\_ratio + 0.370 \cdot I - 0.425 \cdot Battery\_capacity\_ratio + 0.705 \cdot Controller\_Temp + 1.068 \cdot Battery\_Temp + 0.657 \cdot Regulator\_Temp + 0.144 \cdot Ground\_Cable\_Temp + 0.056 \cdot PowerCable\_Before\_Temp + 0.028 \cdot PowerCable\_After\_Temp + 0.004$
$h_3 = f(z)$
Hidden Neuron h_4
$z = -0.611 \cdot V\_ratio + 0.109 \cdot I - 0.109 \cdot Battery\_capacity\_ratio + 0.139 \cdot Controller\_Temp + 0.163 \cdot Battery\_Temp + 0.215 \cdot Regulator\_Temp + 0.485 \cdot Ground\_Cable\_Temp + 0.626 \cdot PowerCable\_Before\_Temp + 0.738 \cdot PowerCable\_After\_Temp - 0.116$
$h_4 = f(z)$
Hidden Neuron h_5
$z = -1.655 \cdot V\_ratio - 0.875 \cdot I + 0.229 \cdot Battery\_capacity\_ratio - 0.338 \cdot Controller\_Temp - 0.485 \cdot Battery\_Temp + 0.582 \cdot Regulator\_Temp + 0.591 \cdot Ground\_Cable\_Temp + 0.851 \cdot PowerCable\_Before\_Temp + 1.036 \cdot PowerCable\_After\_Temp - 1.385$
$h_5 = f(z)$

3. Output Layer – 3 Neurons (Activation: Identity)
$Main\_Switch\_Temp = 0.781 \cdot h_1 + 0.686 \cdot h_2 - 0.032 \cdot h_3 + 0.017 \cdot h_4 + 0.392 \cdot h_5 - 0.340$
$Connector\_Temp = -0.844 \cdot h_1 + 0.836 \cdot h_2 - 0.403 \cdot h_3 + 0.976 \cdot h_4 + 1.941 \cdot h_5 - 0.504$
$Motor\_Cable\_Temp = 0.587 \cdot h_1 + 0.248 \cdot h_2 + 0.779 \cdot h_3 - 0.405 \cdot h_4 + 0.664 \cdot h_5 - 0.365$

The integration of thermal imaging with ANN predictions constitutes another strength of this work. Infrared heat maps confirmed the presence of localized heating in the main switch and connector regions, supporting the choice of prediction targets and validating model outputs. Such spatially resolved imaging adds an important empirical layer to predictive maintenance strategies, complementing the temporal accuracy of ANN forecasts. Moreover, observed thermal gradients between upstream and downstream sections of the main cable echoed patterns reported in insulation degradation studies involving crosslinked polyethylene materials [3,6], suggesting broader implications for long-term system durability.

Despite these strengths, several limitations warrant consideration. The dataset employed was relatively small and collected under controlled laboratory conditions, with no validation in real-world driving environments. This controlled setup may limit generalizability, as field conditions involve more complex interactions such as ambient temperature fluctuations, vibration, and intermittent load cycles. Furthermore, while the ANN demonstrated high predictive accuracy in the tested scenarios, its resilience under conditions of component aging, material degradation, or extreme environmental stressors remains unverified. Future research should therefore prioritize field-based validation, incorporation of larger and more diverse datasets, and exploration of hybrid architectures that integrate physics-informed constraints with data-driven learning.

Therefore, the lightweight ANN demonstrated outstanding performance in predicting critical temperature profiles across EV power cable systems, outperforming SVM and linear regression models both in accuracy and scalability. By identifying battery temperature and post-switch cable temperature as key predictors, the model not only achieved strong empirical alignment with thermal imaging but also provided interpretable insights into system-level thermal dynamics. While limitations in dataset scale and field validation remain, the results strongly indicate that ANN-based frameworks hold promise for embedded deployment in real-time monitoring and predictive maintenance applications in electric mobility.

4 Conclusion

This study demonstrated the capability of a lightweight artificial neural network (ANN) to accurately predict thermal behavior across high-current Electric Vehicle (EV) power cable systems. By integrating electrical and thermal features, the ANN consistently achieved R^2 values above 0.96 and maintained prediction errors within ±2.5 °C, surpassing the performance of support vector machine (SVM) and linear regression models. A key advantage of the ANN is its ability to predict multiple thermal outputs simultaneously, offering efficiency and scalability for real-time applications. Feature importance analysis and thermal imaging confirmed battery temperature and main switch temperature as the dominant predictors, highlighting their role in localized heating and system reliability. While the findings establish strong potential for ANN-based monitoring frameworks, limitations related to dataset size, controlled laboratory conditions, and lack of field validation must be addressed in future work. Expanding datasets and testing under real-world operational conditions will be critical for enhancing generalizability and advancing predictive maintenance strategies in EV thermal management.

Nevertheless, the evaluation framework in this study relied on R^2, MSE, and RMSE metrics calculated from the available dataset, without additional cross-validation or statistical error bars. While these measures provide a comprehensive overview of predictive accuracy, they do not fully capture uncertainty ranges or fold-wise variability. Future work should therefore expand the statistical robustness of the analysis by incorporating k-fold cross-validation, confidence intervals, and larger, more diverse datasets under real-world conditions. Such extensions will enhance the generalizability of the results and support the broader deployment of ANN-based predictive maintenance strategies in EV thermal management.

This work is supported by-Bina Nusantara University as a part of Bina Nusantara University's BINUS International Research – Thermal Management System for High Current Power Cables in Electric Vehicle with contract number: No.081/VRRTT/IV/2025 and contract date: 25 April 2025.

Safarudin Gazali Herawan: Writing – concepts – original draft & review. Azqy Nur Farenzy Saputra, Sharon Yemima, Bangkit Pramesta Yulianto, Henry Ananda Chang: Experimental setup – data collection. Heri Ngarianto, Rida Zuraida, Mohd Zaid Bin Akop: Writing – checking & review.

https://zenodo.org/records/16614762.

During the preparation of this work, the authors used ChatGPT to enhance the clarity of the writing. After using the ChatGPT, the authors reviewed and edited the content as needed and took full responsibility for the publication's content.

References

1. H. Liu, L. Jiao, H. Lin, and L. Li, Design and Application Research of Portable Reversible Thermochromic Patches in Grid Power Supply Systems. Aip Advances. **14**, no. 4 (2024). doi: 10.1063/5.0189608
2. W. Wang, X. Yan, S. Li, L. Zhang, J. Ouyang, and X. Ni, Failure of Submarine Cables Used in High-voltage Power Transmission: Characteristics, Mechanisms, Key Issues and Prospects. Iet Generation Transmission & Distribution. **15**, no. 9, pp. 1387–1402 (2021). doi: 10.1049/gtd2.12117
3. A. S. Alghamdi and R. K. Desuqi, A Study of Expected Lifetime of XLPE Insulation Cables Working at Elevated Temperatures by Applying Accelerated Thermal Ageing. Heliyon. **6**, no. 1, p. e03120 (2020). doi: 10.1016/j.heliyon.2019.e03120
4. Y. Li, Z. Peng, D. Xu, S. Huang, Y. Gao, and Y. Li, Research on the Thermal Aging Characteristics of Crosslinked Polyethylene Cables Based on Polarization and Depolarization Current Measurement. Energies. **17**, no. 10, p. 2274 (2024). doi: 10.3390/en17102274
5. E. E. Sherkawy, L. Nasrat, and M. Rihan, The Effect of Thermal Ageing on Electrical and Mechanical Properties of Thermoplastic Nanocomposite Insulation of Power High-Voltage Cables. Electrical Engineering & Electromechanics. **3**, pp. 66–71 (2024) doi: 10.20998/2074-272x.2024.3.09
6. B. C. Kok, M. Looi, and H. H. Goh, Insulated Gate Bipolar Transistor Failure Analysis in Overvoltage Condition. Renewable Energy and Power Quality Journal. **10**, no. 4 (2024). doi: 10.24084/repqj10.392
7. P. Sun, Z. Li, W. Sima, T. Yuan, M. Yang, K. Fan, X. Chen, and W. Pang, Morning Glory-Inspired Dual-Function Microcapsules for the Self-Reporting and Self-Healing of Electrothermal-Induced Damage of Electrical Devices. Acs Applied Materials & Interfaces. (2024). doi: 10.1021/acsami.3c18483
8. D. Ma, Y. Liu, L. Zheng, J. Gao, Z. Gao, and Z. Zhang, Prediction of Thermally Induced Failure for Electronic Equipment Based on an Artificial Olfactory System. Measurement Science and Technology. **32**, no. 3, p. 035103 (2020). doi: 10.1088/1361-6501/abc9fa
9. E. Mustafa, R. S. A. Afia, and Z. Á. Tamus, Dielectric Loss and Extended Voltage Response Measurements for Low-Voltage Power Cables Used in Nuclear Power Plant: Potential Methods for Aging Detection Due to Thermal Stress. Electrical Engineering. **103**, no. 2, pp. 899–908 (2020). doi: 10.1007/s00202-020-01121-4
10. L. Jin, Z. Zhou, Y. Li, Z. Zou, and W. Zhao, Hotspot Temperature Prediction of Relay Protection Equipment Based on a Physical-Model-Aided Data-Driven Method. Energies. **17**, no. 4, p. 816 (2024). doi: 10.3390/en17040816
11. V. S. K. Reddy, T. Saravanan, N. T. Velusudha, and T. Selwyn, Smart Grid Management System Based on Machine Learning Algorithms for Efficient Energy Distribution. E3s Web of Conferences. **387**, p. 02005 (2023). doi: 10.1051/e3sconf/202338702005
12. A. Dutt and G. Karuna, Machine Learning Approaches for Fault Detection in Renewable Microgrids. Matec Web of Conferences. **392**, p. 01192 (2024). doi: 10.1051/matecconf/202439201192

13. A. Bouhafs, M. R. Kafi, M. L. Louazene, B. Rouabah, and H. Toubakh, Fault-Detection-Based Machine Learning Approach to Multicellular Converters Used in Photovoltaic Systems. Machines. **10**, no. 11, p. 992 (2022). doi: 10.3390/machines10110992
14. T. T. Ağır, Using Machine Learning Algorithms for Classifying Transmission Line Faults. Dümf Mühendislik Dergisi. (2022). doi: 10.24012/dumf.1096691
15. S. Rodrigues, G. Mütter, H. G. Ramos, and F. Morgado-Dias, Machine Learning Photovoltaic String Analyzer. Entropy. **22**, no. 2, p. 205 (2020). doi: 10.3390/e22020205
16. K. Barrera, Á. Sapena-Bañó, J. Martínez-Román, and R. Puche-Panadero, Implementing Deep Learning Models in Embedded Systems for Diagnosis Induction Machine. International Journal of Electrical and Computer Engineering Research. **3**, no. 1, pp. 7–12 (2023). doi: 10.53375/ijecer.2023.319
17. D. Gutiérrez-Rojas, I. T. Christou, D. T. Dantas, A. Narayanan, P. H. J. Nardelli, and Y. Yang, Performance Evaluation of Machine Learning for Fault Selection in Power Transmission Lines. Knowledge and Information Systems. **64**, no. 3, pp. 859–883 (2022). doi: 10.1007/s10115-022-01657-w
18. M. H. Hamdan and D. C. Roach, The Sigmoid Neural Network Activation Function and Its Connections to Airy's and the Nield-Kuznetsov Functions. **2**, pp. 108–114 (2022). doi: 10.37394/232020.2022.2.13
19. Y. V. Khodnevych and D. V. Stefanyshyn, Do We Need a More Sophisticated Multilayer Artificial Neural Network to Compute Roughness Coefficient?. Environmental Safety and Natural Resources. **48**, no. 4, pp. 170–182 (2023). doi: 10.32347/2411-4049.2023.4.170-182
20. M. H. Farrell, T. Liang, and S. Misra, Deep Neural Networks for Estimation and Inference. Econometrica. **89**, no. 1, pp. 181–213 (2021). doi: 10.3982/ecta16901
21. R. Sharma and S. Hosder, Mission-Driven Inverse Design of Blended Wing Body Aircraft With Machine Learning. Aerospace. **11**, no. 2, p. 137 (2024). doi: 10.3390/aerospace11020137
22. Á. E. M. Zavala, J. E. Macías-Díaz, D. Alba-Cuéllar, and J. A. Guerrero-Díaz-de-León, A Literature Review on Some Trends in Artificial Neural Networks for Modeling and Simulation With Time Series. Algorithms. **17**, no. 2, p. 76 (2024). doi: 10.3390/a17020076